Effects of Aerosol Solubility and Regeneration on Warm-Phase Orographic Clouds and Precipitation Simulated by a Detailed Bin Microphysical Scheme

LULIN XUE

National Center for Atmospheric Research, Boulder, Colorado*

AMIT TELLER

The Cyprus Institute, Nicosia, Cyprus

ROY RASMUSSEN

National Center for Atmospheric Research, Boulder, Colorado*

ISTVAN GERESDI

University of Pécs, Pécs, Hungary

ZAITAO PAN

Saint Louis University, St. Louis, Missouri

(Manuscript received 24 March 2010, in final form 14 May 2010)

ABSTRACT

This study evaluates the possible impact of aerosol solubility and regeneration on warm-phase orographic clouds and precipitation. The sensitivity evaluation is performed by simulating cloud formation over two identical 2D idealized mountains using a detailed bin microphysical scheme implemented into the Weather Research and Forecasting model (WRF) version 3. The dynamics, thermodynamics, topography, and microphysical pathways were designed to produce precipitating clouds in a linear hydrostatic mountain wave regime. The cloud over the second mountain is affected by regenerated aerosols advected from the cloud over the first mountain. Effects of aerosol solubility and regeneration were investigated with surface relative humidity of 95% and 85% for both clean and polluted background aerosol concentrations.

Among the findings are the following: 1) The total number of cloud drops decreases as the aerosol solubility decreases, and the impacts of aerosol solubility on cloud drops and precipitation are more significant in polluted clouds than in clean clouds. 2) Aerosol regeneration increases cloud drops and reduces the precipitation by 2%–80% in clouds over the second mountain. Regenerated aerosol particles replenish one-third to two-thirds of the missing particles when regeneration is not considered. 3) Different size distributions of regenerated aerosol particles have negligible effect on clouds and precipitation except for polluted clouds with high aerosol solubility. 4) When the solubility of initial aerosol particles decreases with an increasing size of aerosol particles, the modified solubility of regenerated aerosol particles increases precipitation over the second mountain.

1. Introduction

Atmospheric aerosol acting as cloud condensation nuclei (CCN) and ice nuclei (IN) affect cloud macrophysical and microphysical properties, influence precipitation types and amount, and eventually impact the climate system through the interactions between clouds and precipitation.

* The National Center for Atmospheric Research is sponsored by the National Science Foundation.

Corresponding author address: Lulin Xue, National Center for Atmospheric Research, Boulder, CO 80301.
E-mail: xuel@ucar.edu

DOI: 10.1175/2010JAS3511.1

Under conditions of equivalent liquid water content, increased concentrations of atmospheric aerosol will result in higher concentrations of cloud droplet and thus higher cloud albedo. This so-called aerosol first indirect effect is potentially the largest negative forcing and the most uncertain agent among all radiative forcing components to climate change (Solomon et al. 2007). The effect of aerosol particles on clouds in a dynamically evolving system that includes feedbacks such as aerosol-induced modifications to precipitation is considered as the aerosol second indirect effect (Solomon et al. 2007). On the other hand, aerosol particles are modulated by clouds and precipitation. Processed and transported by clouds, aerosol particles are redistributed in the air through scavenging (sink) and evaporation (source). Their chemical and hygroscopic features are changed by clouds as well (Flossmann 1997). These redistributed and modified aerosol particles affect clouds and precipitation and their subsequent developments (Wurzler et al. 2000).

Atmospheric aerosols play an important role in the fully coupled and highly interactive aerosol–cloud–precipitation–climate system. The problem of how changes in clouds, precipitation, and dynamics are attributed to perturbations in aerosol properties has been extensively studied. For example, the problem of whether or not increases in aerosol loading will result in more precipitation has been under debate for a long time. Controversial results from observational and modeling studies have been documented (e.g., Rosenfeld 2000; Ayers 2005; van den Heever et al. 2006; Teller and Levin 2006). All these studies try to quantify the aerosol effects on clouds and precipitation without considering their feedbacks on aerosols. In contrast, the extent to which changes in clouds, precipitation, and dynamics regulate aerosol has not been extensively studied yet.

Pruppacher and Jaenicke (1995) estimated that globally, clouds evaporate five times before they precipitate. Hence, these evaporating clouds release significant amount of aerosol particles comparable to those generated by oceans and deserts. These regenerated aerosol particles likely affect subsequent development of clouds and precipitation. Experiments and observations proved the existence of in-cloud production of the aerosol sulfate (e.g., Laj et al. 1997; Hobbs 1993, chapter 2). A recent field program, the Cumulus Humilis Aerosol Processing Study (CHAPS), has been conducted to investigate cloud processing of aerosol particles in the vicinity of Oklahoma City (Berg et al. 2009).

The complexities and uncertainties associated with observational studies of aerosol–cloud–precipitation interactions justify the use of numerical models. Many numerical studies have shown that the presence of SO_2 chemistry in the model would not significantly change the cloud properties and precipitation in different kinds of clouds (e.g., Flossmann 1997; Feingold and Kreidenweis 2002; Yin et al. 2005). However, the importance of such processes is that the chemistry changes the hygroscopic character of the aerosol and further facilitates secondary cloud formation. Wurzler et al. (2000) gave a detailed treatment of how mineral dust particles are coated with sulfate by cloud processing. These coated mineral particles then act as giant CCN (GCCN) that can change subsequent cloud development.

Orographic clouds and their potential precipitation are essential for agriculture and the hydrology of watersheds in many regions of the world (Roe 2005). Several features make the orographic precipitating cloud a great candidate for numerical studies of aerosol–cloud–precipitation interactions, such as the relatively weak and organized dynamics, the sensitivity to aerosol characteristics due to the constrained time available to form precipitation in rising air parcels, and the inconclusive estimates of the aerosol effects on orographic clouds and precipitation from observations. Many recent numerical simulations of orographic precipitation showed that the amount of orographic precipitation is sensitive to the available CCN (e.g., Thompson et al. 2004; Lynn et al. 2008; Khain et al. 2008; Muhlbauer and Lohmann 2008) and to the aerosol solubility (Geresdi and Rasmussen 2005). None of them considered both the possible effects of aerosol solubility and regeneration on subsequent clouds and precipitation. Some numerical studies (e.g., Yin et al. 2005; Engström et al. 2008) investigated how aerosol particles are released by evaporated drops and their effects on primary convective clouds and precipitation; however, no systematic sensitivity study has been conducted for regenerated aerosol effects on orographic clouds and precipitation.

Since orographic features are typically complex with multiple ridges (the Alps, Sierra Madre, Rocky Mountains, etc.), it is important to examine the impact of cloud processed aerosol particles by multiple cycles of cloud formation on subsequent cloud and precipitation formation. By simulating idealized cloud formation over two identical two-dimensional (2D) mountains, this study explores the sensitivity of cloud properties, precipitation, and different microphysical processes in warm-phase orographic clouds to changes in aerosol solubility, regenerated aerosol size distributions, and the solubility of regenerated aerosol particles. A detailed bin microphysical scheme coupled with the Weather Research and Forecasting model (WRF) was used to simulate cloud and precipitation formation with surface relative humidity (RH) of 95% (wet) and 85% (dry) for clean and polluted conditions. We attempt to shed light on the following scientific questions:

- To what extent are clean and polluted clouds and precipitation affected by aerosol solubility?
- Does consideration of the aerosol regeneration process make a difference to warm-phase orographic cloud features, precipitation amount, and ambient aerosol concentration?
- How do clean and polluted clouds and precipitation respond to different size distributions of regenerated aerosol particles?
- How does modified solubility of regenerated aerosol particles as a result of cloud processing impact subsequent cloud and precipitation development?

This paper is structured as follows: The detailed bin microphysical scheme, aerosol activation, and regeneration mechanisms are described in section 2, and its implementation into WRF is present in section 3. Results are provided in section 4 followed by a summary and conclusions in section 5.

2. Description of the detailed bin microphysical scheme in WRF

WRF is one of the most widely used public-domain prognostic models in the atmospheric science community. This model was designed to improve forecast quality and investigate meteorological features across scales from turbulence within clouds to global circulations. A number of options are available for boundary layer schemes, cloud and precipitation treatments, and radiative transfer. In-depth descriptions of WRF can be found in published documentation (e.g., Skamarock et al. 2008).

The default microphysical schemes in WRF are all based on bulk parameterizations. The problems being investigated here require detailed descriptions of aerosol and drop size distributions that cannot be represented by these bulk schemes. Therefore, a detailed bin microphysical scheme (Geresdi 1998; Rasmussen et al. 2002) has been implemented in WRF version 3 to study the effects of aerosol solubility and regeneration on clouds and precipitation. The hydrometeor and aerosol microphysical processes in this scheme are described below.

a. Warm-phase microphysics

This detailed bin scheme applies the multimoment conservation technique (Tzivion et al. 1987; Reisin et al. 1996) to ensure the conservation of mass concentration (mixing ratio) and number concentration over 36 mass bins for the following species: cloud and rainwater drops, pristine ice crystals, snowflakes, and graupel particles. The multimoment conservation technique can accurately model the evolution of hydrometeor size distribution by preventing the numerical diffusion–induced artificial broadening of the distribution (Tzivion et al. 1987, 1999). For the purpose of this study, all the ice-phase microphysical processes in this scheme have been switched off. Thirty-six mass doubling bins covering a radius range of 1.56 μm–6.4 mm are used to describe the evolution of the size distribution of water drops. In this study, cloud droplets are defined as drops with radius less than 40 μm and drops with radius greater than or equal to 40 μm are classified as rain drops. The time step for calculating the diffusional growth (condensation and evaporation) of the water drops is 2 s, while for the other processes the same time step as in the dynamics is applied, which in this case is 10 s. The terminal velocities of water drops are calculated using the Best and Bond number approach as described in Pruppacher and Klett (1997). The efficiencies for drop–drop collision–coalescence (C–C) are derived from the tabulated data of Hall (1980). The breakup of water drops induced by collision (Feingold et al. 1988) is treated as well. The nucleation of cloud droplets was originally calculated from an empirical formula of CCN cumulative concentration as a function of supersaturation over the flat water surface (Rasmussen et al. 2002). This process has been updated in this study.

b. Aerosol activation and regeneration

Aerosol activation or cloud droplet nucleation is treated here by calculating the supersaturation and critical radius according to Köhler theory (Pruppacher and Klett 1997). This approach explicitly takes into account the effect of aerosol size distribution on drop size distribution and depletion of aerosol particles in contrast to the more simple technique used in Rasmussen et al. (2002). Thus, 40 more aerosol size bins are added to describe the size distribution of aerosol in the radius range 0.006–66.2 μm. However, in this study, the upper size limit for the initial aerosol distribution is prescribed as 5.2 μm. Regenerated aerosol particles are allowed to grow to 10.4 μm. The assumption that regenerated aerosols can grow to 10 μm is based on the fact that the average radius of completely evaporated drops ranges from 10 to 19 μm for clean clouds and from 6 to 16 μm for polluted clouds based on the simulation results. Taking into account the deviation of the evaporated drop spectrum, drops larger than 25 μm can completely evaporate, which is big enough to release 10-μm radius aerosol particles. We assume that aerosol particles are internal mixtures of soluble material (ammonium sulfate) and insoluble material with a prescribed mass-based solubility.

For each grid point and time step, the model calculates the critical soluble mass for aerosol activation and initiates water drops with appropriate mass following a method similar to the one used in Yin et al. (2000) and

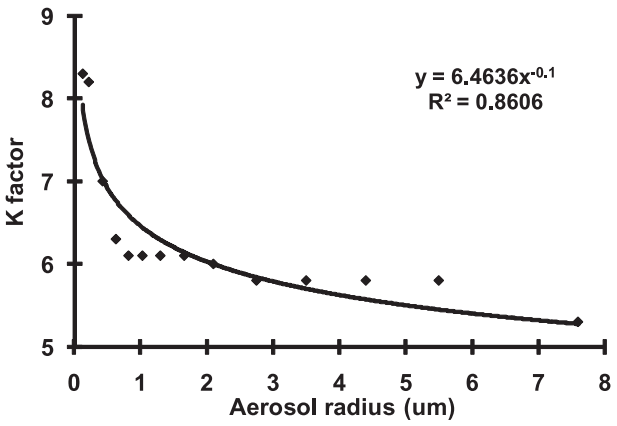

FIG. 1. Aerosol radius vs κ factor. The diamond dots represent the data from Kogan (1991).

Kogan (1991). In this study, the water mass condensed on an aerosol particle with the soluble mass less than 1.25×10^{-17} kg (equivalent radius less than 0.12 μm) is equal to the mass of the first water drop bin. For larger aerosol particles, Kogan (1991) assumed that the droplet is a factor $k(r)$ of the aerosol size (Fig. 1), which is smaller than its equilibrium radius at 100% relative humidity. Therefore, the water mass condensed on aerosol particles with equivalent soluble mass is calculated based on this relation and the activated drops are moved into appropriate bins according to their mass. For instance, given an aerosol particle with 2-μm radius having a mass-based solubility of 12.5%, the soluble material accounts for 1/8 of the aerosol mass and the equivalent radius of the soluble part is 1 μm. The water drop that the soluble part can activate in this case is 6.5 μm according to Fig. 1. Thus, the mass of the actual activated water drop is the sum of aerosol mass and the water mass condensed on it. This water drop is then moved to the appropriate bin for subsequent microphysical processes. Here, we assume the soluble and insoluble parts of aerosol particles have the same density.

When the solubility is taken into account, the definition of GCCN as a certain size aerosol (such as $r > 1$ μm) is no longer appropriate. We propose to define GCCN as aerosol particles that can directly activate water drops with radii greater than 5 μm. Therefore, the small solubility associated with large aerosol particles implies lower GCCN concentration than that of larger solubility particles.

In addition to the aforementioned explicit aerosol activation submodule, the aerosol regeneration mechanism has been implemented in the current version of the bin microphysical scheme. As mentioned earlier, the diffusional growth on water droplets is calculated using a ''sub-time step'' of 2 s. Within each 2-s time step, the condensation or evaporation changes the size distribution of the water drops in a certain grid box. When the drops in a grid box experience evaporation, the number concentration reduces. The difference in number concentration represents the number of completely evaporated drops. Mitra et al. (1992) showed that when evaporation occurs, one water drop usually releases one aerosol particle. Therefore, these newly evaporated drops release as many aerosol particles back to the same grid box at the end of the 2-s time step. Once this total number of regenerated aerosol is known, the size distributions of these aerosol particles can be constructed by applying different functions such as gamma and lognormal functions. Wurzler et al. (2000) found that when processed by clouds, the aerosol particles become more hydrophilic. Thus, the solubility of regenerated aerosol particles can be adjusted in the scheme to account for this effect.

It is worth mentioning that for a certain water drop bin, the change in number concentration is attributed to the gain from the residues of evaporated drops from larger bins and to the loss of droplet mass by evaporation in the current bin. So, the exact number of completely evaporated drops in each bin is unknown. Therefore, the total number of evaporated drops in a grid box can only be calculated as the difference between two integrals of number distributions before and after evaporation. This is also the reason that we cannot assume a direct relation between the regenerated aerosol size and the size of the evaporated drop.

c. *Aerosol scavenging*

Through activation, aerosol particles are depleted by drops falling on the ground, which is the so-called nucleation scavenging. Removal of aerosol particles by rain drops due to gravitational collision is called the impaction scavenging. Flossmann et al. (1985) showed that the aerosol mass scavenged by the in-cloud impaction scavenging is smaller by several orders of magnitude than that removed by nucleation scavenging. Since orographic clouds form along the surface, the below-cloud impaction scavenging is insignificant. Aerosol particles can also enter drops through Brownian motion and thermophoresis. Geresdi and Rasmussen (2005) found that the aerosol scavenged by the Brownian and phoretic collections is negligible in orographic clouds similar to those in our study. Dry deposition of supermicron aerosol is another mechanism through which aerosol particles are removed from the atmosphere. In this study, the upper limit of aerosol radius is 10.4 μm, which has a terminal velocity of about 2.5 cm s^{-1}. A brief calculation shows that an aerosol particle with 10.4-μm radius and another with 5.2-μm radius released from the first cloud will fall respectively about 600 and 150 m in the vertical before they are caught by the updraft in the second cloud.

Considering that the cloud depth is around 3–4 km (see section 4) and most aerosol particles are smaller than 5.2 μm, we believe that the dry deposition is not important to the simulations. Therefore, the impaction scavenging, the Brownian and phoretic scavenging, and dry deposition of aerosol particles are not considered in this study.

3. Approach

Since we used a detailed bin microphysical scheme in this study, the extremely high cost of running the model in three-dimensional (3D) domains leads us to a less costly 2D approach. Although 2D simulation cannot resolve the dynamics and energetics as accurately as 3D simulation (such as flow pattern, convergence–divergence, energy cascade, etc.), it is sufficient to provide a reasonable dynamic framework for the detailed physical process study performed here. Thus, in order to understand the possible effects of aerosol solubility and regeneration on warm-phased orographic clouds, idealized 2D simulations of moist flows over two bell-shaped mountains have been conducted. The model setups in this study are the same as case 1 of the Seventh World Meteorological Organization (WMO) International Cloud Modeling Workshop (Morrison et al. 2009) except that two bell-shaped mountains are used in this study instead of one. Muhlbauer et al. (2010) presents an intercomparison study of this case on how aerosol concentrations influence the orographic precipitation distribution and dynamics by simulating mixed-phase clouds using three dynamic frameworks coupled with three microphysical schemes respectively. Muhlbauer and Lohmann (2008) provided a detailed investigation on the same issue by simulating warm-phased clouds using similar setups. This study used the weak dynamics setups of this WMO cloud modeling workshop case to examine the relation between aerosol properties and cloud microphysics. The model domain, topography, dynamics, thermodynamics, aerosol initializations, and the experimental design are summarized in the following subsections.

a. Model configurations

The 2D domain consists of 400 grid points in the horizontal with a resolution of 2 km. There are 60 terrain-following vertical levels in the domain reaching the model top at 23 km. The vertical resolution varies from 20 m at the lowest layer to about 1400 m at the highest layer. A Rayleigh damping sponge layer is applied in the upper 10 km of the computational domain to minimize reflections of vertically propagating gravity waves from the rigid upper model boundary. A free-slip condition is imposed at the lower model boundary. Two identical bell-shaped mountains are located at 200 and 500 km with peak height of 800 m and half-width of 20 km [$h_0 = 800$ m, $a = 2 \times 10^4$ m in Eq. (20) from Muhlbauer and Lohmann (2008)]. The soundings used to initialize the idealized 2D model are shown in Fig. 2. The solid line indicates the temperature and the dashed lines indicate the dewpoint temperatures for the two relative humidities. The surface temperature is set to 280.15 K and the relative humidities are set to 0.95 (long dashed line) and 0.85 (short dashed line). The profile of the relative humidity is prescribed by the function

$$\mathrm{RH}(z) = a + \frac{b - a}{1 + \exp[-c(z - z_0)]}, \tag{1}$$

with $a = 0.95$ for the wet condition and $a = 0.85$ for the dry condition, $b = 0.03$, $c = 0.0015\ \mathrm{m}^{-1}$, and $z_0 = 6000$ m. The horizontal wind U is prescribed unidirectionally with a constant value of 15 m s^{-1} below 10 km increasing linearly above that level with approximately $\partial U/\partial z = 1.84\ \mathrm{m\ s^{-1}\ km^{-1}}$. A Smagorinsky first-order closure was used for turbulence. Monotonic flux limiters for advection of scalars (Wang et al. 2009) have been used in the simulations. Because of the very fine vertical resolution close to the ground, the boundary layer parameterizations are switched off to exclude numerical difficulties. The effect of radiative cooling on drizzle formation of orographic clouds was investigated in Rasmussen et al. (2002). Their results showed that a very small effect was found only in the case of polluted clouds. Thus, the radiation schemes are turned off to reduce the complexity of this aerosol–cloud–precipitation interaction study.

The aerosol initial background concentrations are prescribed as clean and polluted to test the aerosol effects under two extreme conditions (Fig. 3). Both distributions consist of three modes of lognormal distributions superimposed on a background distribution (Jaenicke 1988). As mentioned in section 2b, the radius spectrum shown in Fig. 3 ranges from 0.006 to 5 μm (r_a). The number concentrations of the whole size range in the first model level are 122.3 cm^{-3} for clean air (N_C) and 9.23×10^4 cm^{-3} for polluted air (N_P). For $r_a > 0.05$ μm, $N_C = 72.8$ cm^{-3} and $N_P = 5659$ cm^{-3}. For $r_a > 0.1$ μm, $N_C = 57.4$ cm^{-3} and $N_P = 1720$ cm^{-3}. For $r_a > 1$ μm, $N_C = 0.33$ cm^{-3} and $N_P = 0.87$ cm^{-3}. The initial aerosol number concentrations are assumed to decay exponentially with height below a certain constant concentration height (Jaenicke 1988). The scale height for both backgrounds is 1000 m and the constant concentration height is 4000 m.

b. Experimental design

The initial dynamics, thermodynamics, and aerosol concentrations are prescribed to generate two consecutive hydrostatic mountain wave clouds. The first cloud

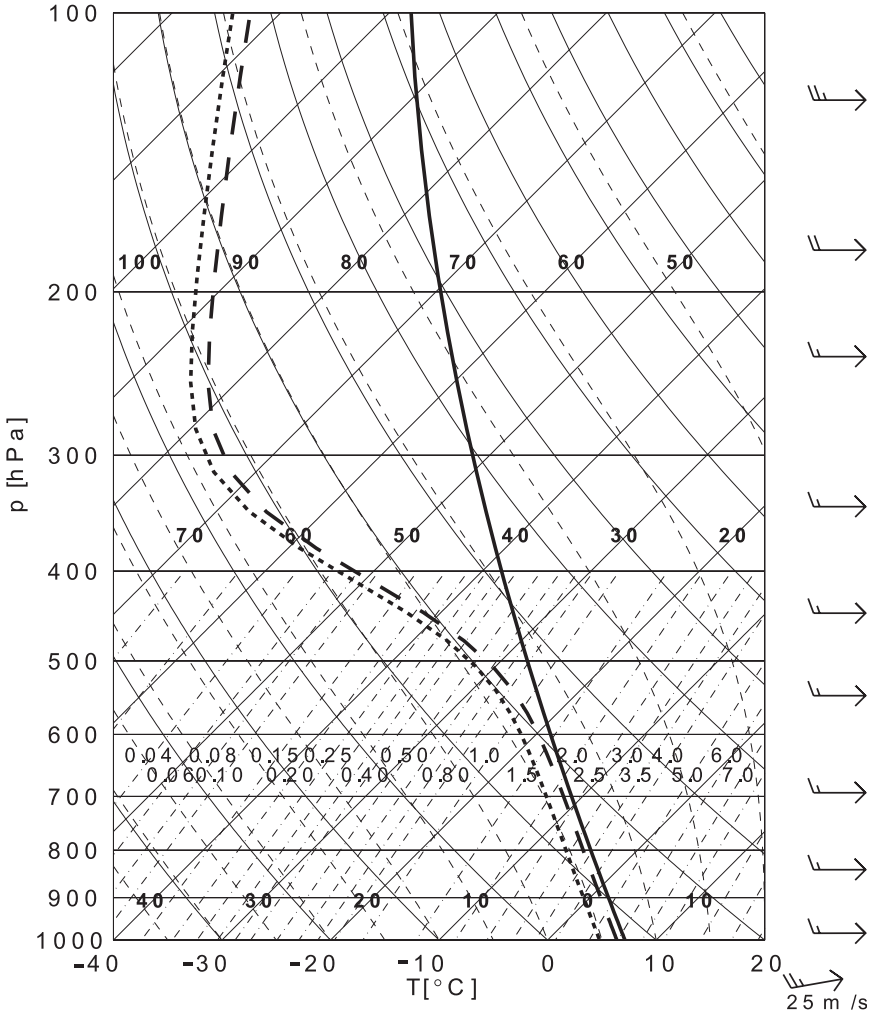

FIG. 2. The atmospheric soundings for the ideal 2D simulations. The temperature is indicated as the solid line with a surface temperature of 280.15 K. The long dashed line indicates the dewpoint temperature with 95% surface RH. The short dashed line is the dewpoint with 85% surface RH. The wind speed is 15 m s^{-1} below 10 km and increases linearly to around 39 m s^{-1} at the domain top.

works as a prototype of cloud processing. The processed and regenerated aerosol particles from the leeward side of this cloud are advected downwind toward the second cloud. Cloud and precipitation features of the first cloud are evaluated for five solubility functions. Four are fixed solubility: 100% (F1), 50% (F05), 10% (F01), and 1% (F001) for all aerosol particles. One has varying solubility as a function of aerosol radius (FC):

$$\mathrm{FC} = \begin{cases} 1 & r \le 5\times10^{-8} \\ 1.13\times e^{-2.5\times10^{6}\times r} & 5\times10^{-8} < r \le 1\times10^{-6} \\ 5\times10^{-10}\times r^{-1.382} & 1\times10^{-6} < r \le 5\times10^{-6} \\ 0.01 & r > 5\times10^{-6} \end{cases}. \quad (2)$$

Here r is the aerosol radius in meters. This formula depicts a monotonic decrease of solubility with the increasing aerosol size. As shown in Fig. 4, this function can describe mixtures of ammonium sulfate in fine mode and dusts in coarse mode. The fixed solubility cases represent aerosol mixtures with certain bulk solubility. As mentioned in section 2b, the different solubility functions determine the CCN and GCCN concentrations given the same aerosol background size distribution. The sensitivities of the second cloud and associated precipitation to three size distributions of these regenerated aerosol particles are then investigated for these different solubility functions.

Among the three size distributions, one is single mode lognormal distributions (SMD), and the others are bimodal

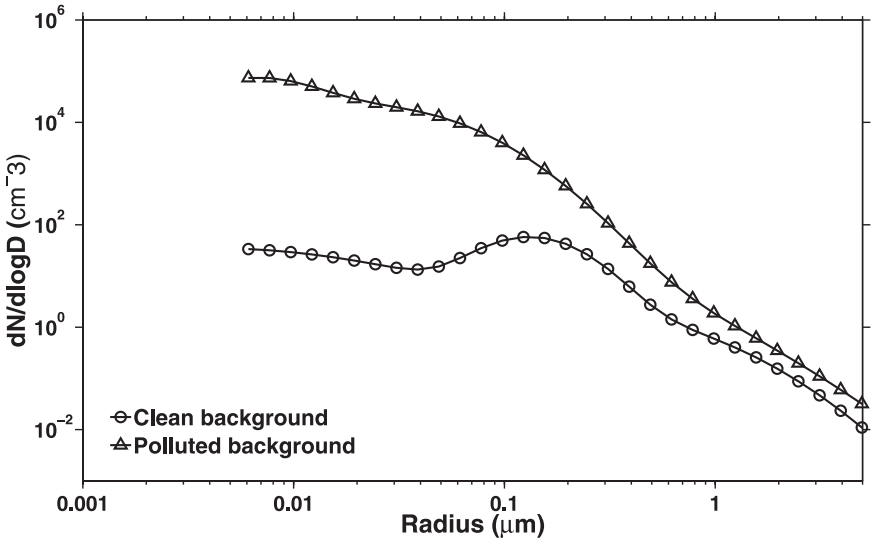

FIG. 3. Size distributions of the clean and polluted aerosol initial concentrations used in the simulations. Both distributions consist of three modes of lognormal distributions (Jaenicke 1988).

lognormal distributions (BMD). SMD and BMD follow Eq. (3) with $m = 1$ and $m = 2$, respectively:

$$\frac{dN(r)}{d(\ln r)} = \sum_{i=1}^{m} \frac{n_i}{\sqrt{2\pi}\,\ln\sigma_i} \exp\left[-\left(\frac{\ln r - \ln\tilde{r}_i}{\sqrt{2}\,\ln\sigma_i}\right)^2\right]. \quad (3)$$

Here r is aerosol radius (μm), $\tilde{r}_i$ and σ_i are respectively the geometrical mean radius (μm) and standard deviation, n_i is the integral of the ith normal distribution, and $N(r)$ is the cumulative aerosol number concentration (cm^{-3}). The three size distributions are described in Table 1.

SMD is a simple distribution that regenerated aerosol can follow. However, when a large $\tilde{r}_1$ or a large σ_1^* is chosen to represent the aerosol growth by the collision–coalescence process (Flossmann et al. 1985), extra arbitrary aerosol mass will be introduced into the domain. For example, when $\tilde{r}_1 \geq 0.3\,\mu$m and $\sigma_1^* \geq 0.3$, there is more than twice the initial aerosol mass at the end of the simulation. Thus, we apply BMD to correct this deficiency. The small mode of BMD is the same as SMD. The number concentration of large mode (n_2) in a grid box at a certain time step is assumed to be 5% of the drop number concentration change caused by the C–C process in the same grid box at the same time step. By applying this relation, we can conserve the aerosol mass and reflect the aerosol growth by the C–C process at the same time. The small mode number concentration (n_1) is thus the difference between the total regenerated aerosol number (N) and n_2.

Since the aerosol solubility does not change after cloud processing once it is independent of the aerosol size (for F1, F05, F01, and F001), modifications of regenerated aerosol solubility can only occur in FC cases in this study. The effects of modified solubility of regenerated aerosol particles on clouds and precipitation have been investigated by two groups of experiments with BMD1 distribution. For clean clouds, the solubility of regenerated aerosol particles greater than 0.05 μm is set to 0.1, which is about the average solubility for all aerosol particles greater than 0.05 μm. For polluted clouds, the solubility of regenerated aerosol particles greater than 0.05 μm is set to the average value at 0.5. For particles smaller than 0.05 μm, the solubility does not change (still is 100%).

Table 2 summarizes all the simulations that have been conducted in this study. The regeneration of aerosol is not considered in the control (CTRL) cases. There are 84 experiments in total to explore the effects of aerosol solubility and regeneration on warm-phase orographic

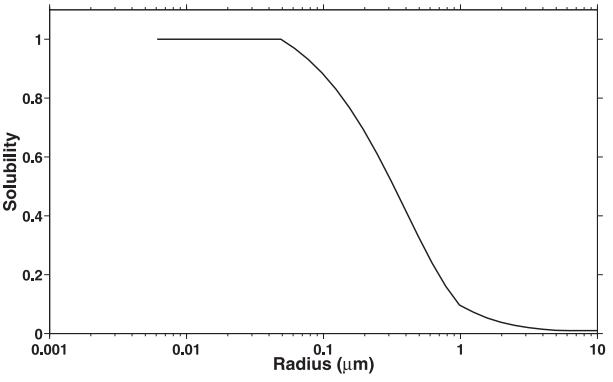

FIG. 4. Aerosol solubility as a function of size (FC).

TABLE 1. Size distributions of regenerated aerosols.

	$\tilde{r}_1(\mu m)$[a]	σ_1^{*b}	$\tilde{r}_2(\mu m)$[a]	σ_2^{*b}	n_2^c
SMD	0.1	0.3	—	—	—
BMD1	0.1	0.3	1.0	0.3	$0.05 \times \Delta N_{C-C}$[d]
BMD2	0.1	0.3	2.0	0.3	$0.05 \times \Delta N_{C-C}$

[a] Median radii for small and large modes, respectively.
[b] The spread parameters ($\sigma_i^* = \log\sigma_i$).
[c] The number concentration of the large mode.
[d] The change of drop number concentration by the C–C process.

clouds and precipitation. Each case has been simulated for 10 h, which is long enough to reach steady state.

4. Results

It has been long understood that under hydrostatic conditions and high enough Froude number an orographic cloud will form on the upslope side of a mountain and tilt upstream with height. Figure 5 illustrates the time-averaged cloud and rain mixing ratios of four CTRL simulations of two orographic clouds with aerosol containing 100% solubility. The cloud tops for both the wet simulations reach about 4-km height whereas the dry runs barely reach 3 km. The cloud bases of the wet clouds are also lower than those of the dry clouds, which can be inferred from the sounding (see Fig. 2). The maximum cloud water mixing ratio approximates 0.7 g kg^{-1} for the first cloud and is about 0.5 g kg^{-1} for the second cloud under the clean condition, which is independent of the moisture condition. For polluted clouds, the first cloud exceeds 0.7 g kg^{-1} under both wet and dry conditions. The second cloud has a maximum cloud water content of 0.9 g kg^{-1} in the wet environment and close to 0.7 g kg^{-1} when the air is dry. The maximum rainwater mixing ratios are 0.32 (0.05) g kg^{-1} and 0.25 (0.12) g kg^{-1} for the first and the second cloud in C_RH95_CTRL_F1 (C_RH85_CTRL_F1). They are 0.12 (<0.01) g kg^{-1} and 0.06 (<0.01) g kg^{-1} for the first and the second cloud in P_RH95_CTRL_F1 (P_RH85_CTRL_F1). As expected, a higher cloud water content and lower rainwater content in the more polluted case has been simulated. The dry condition generates smaller clouds and less rain than the wet condition. The maximum vertical velocity associated with the orographic cloud is about 0.44 m s^{-1} during the cloud formation period and the averaged updraft is 0.25 m s^{-1} (not shown).

a. *Control simulations: Solubility effect of background aerosols on clouds and precipitation over the first hill*

In this section, only the solubility effect of background aerosol on clouds and precipitation over the first hill is investigated. The effect of aerosol regeneration on the second cloud will be discussed in the next section.

TABLE 2. Summary of the experiments.

Case name/solubility	F1	F05	F01	F001	FC
			Wet clean		
C_RH95_CTRL*	×	×	×	×	×
C_RH95_SMD	×	×	×	×	×
C_RH95_BMD1	×	×	×	×	×**
C_RH95_BMD2	×	×	×	×	×
			Dry clean		
C_RH85_CTRL	×	×	×	×	×
C_RH85_SMD	×	×	×	×	×
C_RH85_BMD1	×	×	×	×	×**
C_RH85_BMD2	×	×	×	×	×
			Wet polluted		
P_RH95_CTRL	×	×	×	×	×
P_RH95_SMD	×	×	×	×	×
P_RH95_BMD1	×	×	×	×	×**
P_RH95_BMD2	×	×	×	×	×
			Dry polluted		
P_RH85_CTRL	×	×	×	×	×
P_RH85_SMD	×	×	×	×	×
P_RH85_BMD1	×	×	×	×	×**
P_RH85_BMD2	×	×	×	×	×

* Here C and P stand for the clean and polluted background, RH95 and RH85 indicate the wet and dry condition, CTRL has no regenerated aerosol, and × indicates a combining case has been performed.
** Additional cases for modified solubility of regenerated aerosol particles as described in the text.

The time series of total cloud and rainwater mass reflecting the ability of background aerosol to ''hold'' liquid water in the air are shown in Figs. 6a1,a2 for the wet condition. The water condensed by the polluted background aerosol is about 10% more than that of the clean case. Different solubilities result in about 20% variation of total water for both clean and polluted clouds. On the other hand, the number concentration of cloud drops is strongly dependent on the aerosol solubility. The time series of total number of water drops shown in Figs. 6b1,b2 shows that decreasing the solubility by one order of magnitude (from 100% to 10% and from 10% to 1%) results in about a 40% decrease in the total drop number of clean clouds and a 60% decrease of polluted clouds. The more prominent effect of solubility on cloud drop number in polluted clouds has been pointed out by many other studies (e.g., Feingold 2003; Lance et al. 2004; Geresdi and Rasmussen 2005; McFiggans et al. 2006; Reutter et al. 2009). The similar water mass but very different drop concentrations of clouds regulated by aerosol particles with various solubilities implies that the ability of precipitation formation should be approximately inversely proportional to the drop concentration. This is verified by Figs. 6c1,c2, illustrating the time series of the

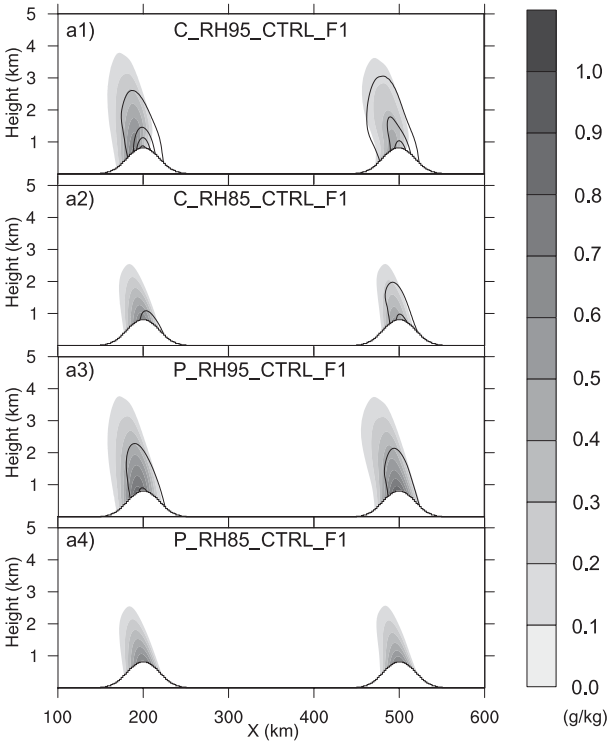

FIG. 5. Time-averaged cloud and rain mixing ratios (g kg^{-1}) of (a1) C_RH95_CTRL_F1, (a2) C_RH85_CTRL_F1, (a3) P_RH95_CTRL_F1, and (a4) P_RH85_CTRL_F1. The shaded areas represent the cloud water. The black contours indicating the rainwater starts at 0.01 g kg^{-1} with an interval of 0.1 g kg^{-1}.

precipitation rate. Having the lowest drop concentration, F001 always generates more precipitation and earlier than others. It is also noticed that polluted clouds with 1% aerosol solubility can generate heavier rain than most clean clouds with higher aerosol solubilities.

Under the dry condition, both clean and polluted clouds have similar water mass which is about 50% of that in the wet condition and the total water mass is insensitive to solubility for both clouds (not shown here). This fact indicates that there exists a threshold of moisture supply below which the cloud mass is not affected by aerosol solubility. The effect of solubility on the total drop number is the same as in the wet condition and the precipitation rates of clean clouds are always greater than those of polluted clouds (not shown).

The ability to examine details of the water drop size distribution is a unique feature of the detailed bin microphysical scheme. The time-averaged drop size spectra of the entire cloud over the first hill are illustrated in Fig. 7 for both clean and polluted clouds in the wet condition. Because of the low colloidal stability of clean clouds, the drop size distributions of clean clouds are broader and insensitive to the aerosol solubility. On the other hand, the size spectra in polluted clouds are narrower and very sensitive to the aerosol solubility. These features persist in the dry condition as well (not shown). To help explain the differences between spectra, three normalized microphysical parameters are introduced. They are 1) the rate of water mass activated by aerosol particles normalized by the number of activated aerosol particles (kg s^{-1}), which represents the average mass or size of the activated drops; 2) the rate of water mass condensed on existing drops normalized by the total number of drops (kg s^{-1}), which indicates the average growth rate of each drop by condensation; and 3) the rate of drop number changed by the C–C process normalized by the total number of drops (s^{-1}), which implies the efficacy of the C–C process.

Figure 8 illustrates the time series of these normalized parameters of the first cloud in the wet condition. It is obvious that high solubility cases (F1 and F05) always have larger activated drops than others because of the higher concentrations of GCCN of these cases (offline calculation shows that GCCN concentrations of F1 and F05 are more than 3 times that of F01 and more than 20 times that of F001). The abundant GCCN activate many large drops, which facilitates the C–C process (Fig. 8c) and results in broad drop size distributions (see Fig. 7). On the other hand, low solubility cases (F01 and F001) always have higher normalized condensation rates than others because of their comparatively lower CCN concentrations. The fewer available CCN in these cases lead to higher supersaturations and stronger condensation rates, which supply a microphysical pathway to generate large drops other than those activated by GCCN. Thus, the C–C process is sustainable in these cases and this maintains broad spectra as well. The very low activation rates and condensation rates of FC cases are caused by the following two reasons: (i) the very small solubility (from 10% to 1%) associated with large aerosol particles (from 1 to 5 μm) of FC cases makes the GCCN concentration much less than those of F1 and F05 cases, and (ii) the high solubility (greater than 50%) of aerosol particles smaller than 0.32 μm results in CCN concentration similar to that of the F1 and F05 cases. As a result, the C–C process is suppressed and the spectra of FC are the narrowest.

Comparison of Figs. 6c and 8c reflects that the C–C process dominates precipitation formation in warm-phase clouds. However, it is the normalized C–C rate—not the absolute C–C rate—that indicates the precipitation efficacy of a cloud. It is found that the absolute C–C rates are greater in polluted clouds than in clean ones when the aerosol solubility is high, while the precipitation rates are lower in polluted clouds. Examination of Fig. 8 shows that the contribution of activation of GCCN to precipitation

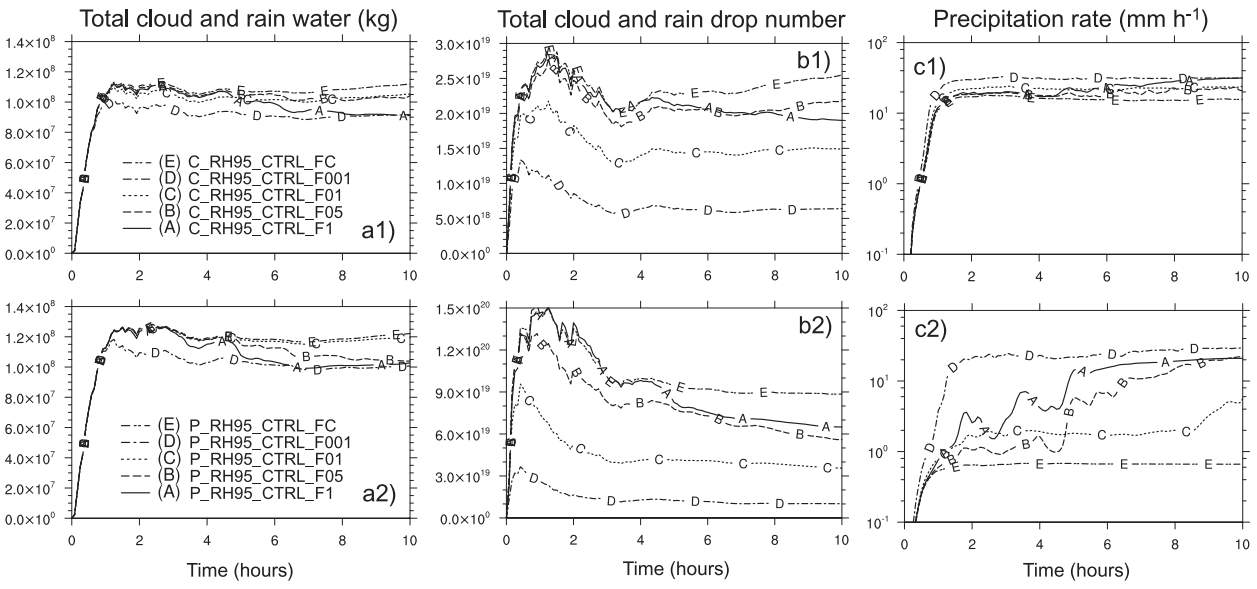

FIG. 6. Time series of (a) total cloud and rainwater (kg), (b) total cloud and rain drop number, and (c) precipitation rate (mm h^{-1}) in logarithmic scale of clouds over the first hill in the wet condition, for (top) clean and (bottom) polluted clouds. Lines A–E represent solubility functions of F1, F05, F01, F001, and FC, respectively.

formation is more significant in polluted clouds than in clean clouds when the aerosol solubility is high (50%–100%).

The dynamics setup of the simulations determines that most of the evaporation occurs on the leeward edge of the cloud, which is downwind of other microphysical processes. After the activation, condensation, and C–C processes shape the cloud within the supersaturated area on the upslope side, cloud drops are advected downwind to the unsaturated area and experience evaporation. Therefore, evaporation is not very important to the precipitation formation in this research. Breakup processes are also negligible in this study because the variation of drop mass and number associated with this process is several orders of magnitude smaller than the other processes.

The effects of aerosol solubility on precipitation over the first hill are summarized in Table 3. The ground total precipitation (GTP) reflects the integration of precipitation rate accurately for each case. F001 cases generate the highest GTP among others given the same aerosol background and humidity condition, whereas FC cases are the lowest. The ratios of GTP between F001 and FC of clean clouds are 1.9 and 3.2 for the wet and dry conditions, respectively. The corresponding ratios of polluted clouds are 34.9 and 4.6. When aerosol solubility reduces from 100% to 10%, the GTP varies little and nonlinearly for clean clouds under both the wet and dry conditions. However, for polluted clouds, the decreasing solubility rapidly reduces GTP in the wet environment and slightly increases it when the condition is dry.

To extend our analyses, we compared the effects of solubility on cloud droplet formation with those of Reutter et al. (2009), who used a cloud parcel model containing a detailed bin microphysical scheme with the κ-Köhler activation method (Petters and Kreidenweis 2007) to investigate the formation of cloud droplets under pyroconvective conditions. Reutter et al. (2009) ran a series of 961 simulations to cover a broad parameter space. They found that three distinct regimes of aerosol activation exist: aerosol-limited (high values of supersaturation and activation fraction of aerosol particles), updraft-limited (low values of supersaturation and activation fraction of aerosol particles), and transitional regimes. The temperature and liquid water content values used to initialize the parcel model in Reutter et al. (2009) are 285.2 K and 0.8 g kg^{-1}, which are close to those of this study (280.15 K and 0.5–0.9 g kg^{-1}). In addition, the parameter space of aerosol and meteorological conditions of this study has been covered by theirs. Therefore, qualitative comparison between the two studies is feasible.

TABLE 3. Ground total precipitation of the first cloud from CTRL cases.

	GTP (mm)				
Case name/solubility	F1	F05	F01	F001	FC
C_RH95_CTRL	211	177	205	284	146
C_RH85_CTRL	22	21	27	58	18
P_RH95_CTRL	107	71	19	216	6.2
P_RH85_CTRL	2.5	2.6	4.0	10	2.2

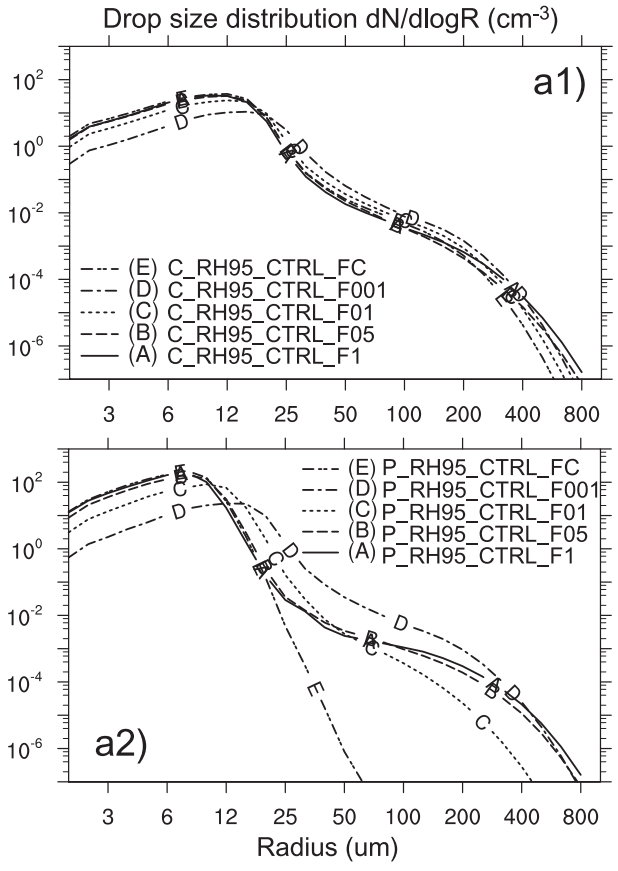

FIG. 7. Time-averaged drop spectra of (a1) clean clouds and (a2) polluted clouds over the first hill in the wet condition.

In this study, the sounding generated an updraft of 0.44 m s^{-1} during the cloud formation stage for each case. The time-averaged updraft is about 0.25 m s^{-1}. Under such updraft, the activation of clean cloud is classified into the aerosol-limited regime because of its very low aerosol concentration (122 cm^{-3}). The activation of polluted cloud is in the updraft-limited regime as the aerosol concentration is much higher (9.23×10^4 cm^{-3}), the supersaturation is small (<0.2%), and the activation fraction is also small (<2.2%). Despite the very different approaches of these two studies—aerosol activation based on hygroscopicity κ versus solubility ϵ, and 1D cloud parcel model versus 2D cloud-resolving model —the results agree with each other qualitatively well. Our results confirmed the findings of Reutter et al. (2009) that the sensitivity of cloud drop number concentration to aerosol solubility (κ in their case) is relatively high when the solubility is very low and in the updraft-limited regime (polluted clouds in this study).

The parcel model used in Reutter et al. (2009) does not incorporate the C–C process partially because their main interest was in cloud droplet activation. This study took one step further to use WRF to simulate the entire cloud system. It is found that when all the warm-phase microphysical processes are taken into account, the sensitivity of cloud drop number concentration to aerosol solubility is higher than that in activation stage (not shown) because of the nonlinear responses of the cloud drop number to the C–C process and the breakup process. This result suggests that the relative importance of aerosol solubility effect on clouds achieved by cloud parcel models may need to be revisited using models with complete dynamics and microphysics.

The analyses performed in this section show that 1) the warm-phase orographic precipitation is significantly affected by aerosol solubility, 2) polluted clouds are more sensitive to aerosol solubility than clean clouds, and 3) clean clouds are more sensitive to aerosol solubility in the dry condition while polluted clouds are more sensitive in the wet condition. To check whether these effects are general to orographic clouds, two extra experiment sets with different Froude numbers have been carried out (one set with 10-km mountain half-width and another with 30-km half-width). The results indicate that the qualitative effects of aerosol solubility on warm-phase orographic clouds documented above are independent of the Froude numbers tested in this study.

b. *Effects of aerosol regeneration on clouds and precipitation over the second hill*

Since the prevailing wind is unidirectional, most of the regenerated aerosol particles released from the evaporated drops in the leeward part of the cloud are advected promptly downwind. Thus, these regenerated aerosol particles do not affect their parent cloud (the first cloud), which should not be too different from the CTRL cases for all sensitivity simulations. In fact, the relative differences of GTP and number of total evaporated drops over the first hill between sensitivity simulations and corresponding CTRL cases are less than 3% throughout this study. Therefore, the vapor supply and the number of regenerated aerosol particles associated with the second cloud can be considered as the same for these cases. At about the fifth hour of the simulation, the advected regenerated aerosol particles from the first cloud encounter the second cloud. Hereafter, we focus on the features of the second cloud, which is strongly affected by these regenerated aerosol particles.

Table 4 lists the GTP of the second cloud for all cases. It is found that given a size distribution of regenerated aerosol particles, the effects of aerosol solubility on precipitation over the second hill are similar to those of CTRL cases over the first hill. However, a decrease from 100% to 10% of aerosol solubility leads to an increase of GTP over the second hill for clean and polluted clouds when aerosol regeneration is considered, which was not

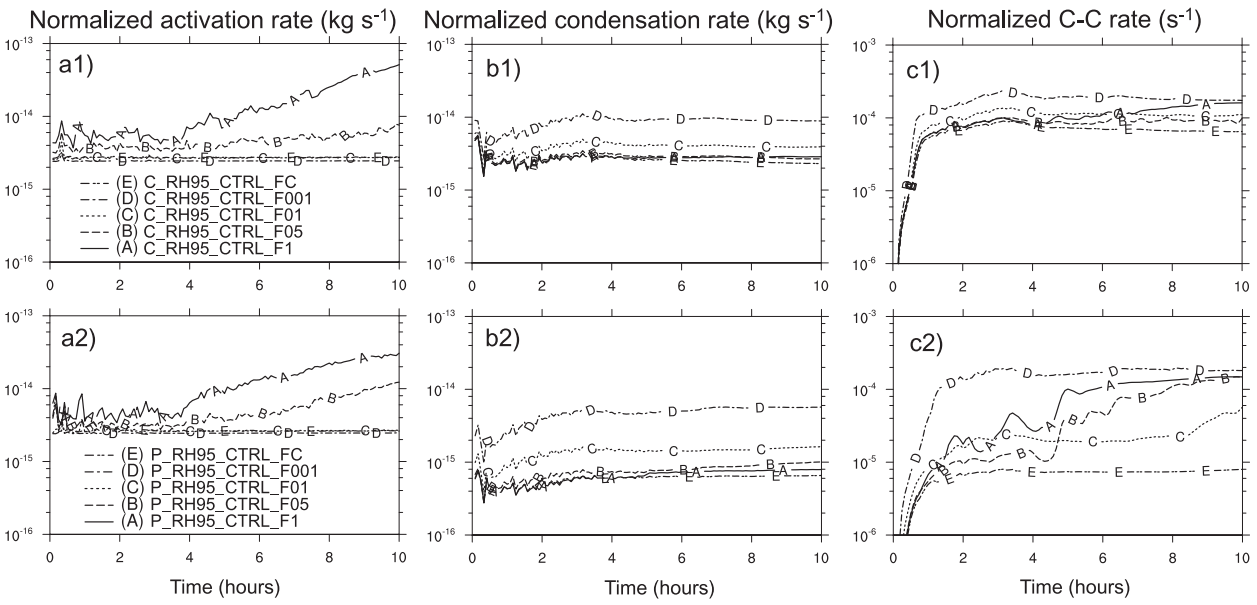

FIG. 8. As in Fig. 6, but for (a) activation rate normalized by the activated aerosol number (kg s^{-1}), (b) condensation rate normalized by the total drop number (kg s^{-1}), and (c) C–C rate normalized by the total drop number (s^{-1}). All values are in logarithmic scale.

observed in CTRL cases over the first hill in the wet condition. Because the amount of aerosol particles released by the first hill is less than the initial aerosol number, the reduced CCN leads to a second cloud with less total drop number than the first cloud of CTRL cases after about 5 h (see Figs. 6, 9, and 10 for reference). Under such conditions, the activation process is suppressed by the reduced GCCN concentration. This effect leads to much less GTP than that in the first cloud of CTRL for the F1 and F05 cases. For the F01 and F001 cases, the efficient condensation process results in as much or even more GTP than in the first cloud of CTRL.

Examination of Table 4 shows that when the solubility of the fine mode aerosol is not very small (F1, F05, F01, and FC), aerosol regeneration reduces the precipitation by 1) about 40% for clean clouds in the wet condition, 2) about 60% for clean clouds in the dry condition, 3) about 70% for polluted clouds in the wet condition, and 4) about 10% for polluted clouds in the dry condition compared to the corresponding CTRL cases. When the solubility is very small (F001), aerosol regeneration reduces the precipitation by less than 20% for both clean and polluted clouds in both the wet and the dry conditions. The precipitation reduction range for both clouds in all kinds of conditions is from 2% to 80%. In the real atmosphere, bulk aerosol solubility ranges between 0.1 and 1 in most occasions. Under such condition, only polluted clouds respond to aerosol solubility sensitively (see Table 4). However, if a pollution plume containing low solubility particles such as metal dust and soot encounters the moist air, a slight change of the composition might result in large difference in rainfall amount. It is also found that when aerosol regeneration is considered, cloud drop number concentration and precipitation are more sensitive to aerosol solubility in general.

We choose the F05, F001, and FC cases to show the effects of size distributions of regenerated aerosol on the second cloud and precipitation. F001 and FC represent the extreme conditions in terms of GTP while F05 is representative of the F1, F05, and F01 cases. Figures 9 and 10 illustrate the time series of total water mass, total number of drops, and precipitation rate of the second clouds for these three solubilities in the wet condition. In addition to cases with aerosol regeneration (SMD, BMD1, and BMD2), CTRL cases are also plotted for reference. It is obvious that CTRL cases have the lowest drop number after 5 h because no regenerated aerosol particles are released from the first cloud. All the newly initiated drops of CTRL cases in the second clouds after 5 h are activated from the interstitial aerosol particles that have not been activated in the first clouds. The more prominent differences in drop number than those in water mass between CTRL cases and other cases with aerosol regeneration result in higher condensation rates and thus higher precipitation rates of CTRL cases than others.

It is noticed that F05 and FC cases have similar cloud structures in terms of water mass and drop number. However, more GCCN associated with BMD distributions of F05 leads to more large drops and thus higher precipitation rates than FC cases (see curves C and D in Figs. 9c and 10c). Unlike F05 and FC cases, F001 has the least drop number in the first cloud and thus releases

TABLE 4. As in Table 3, but for clouds over the second hill from all sensitivity cases. Asterisks represent values of cases with modified solubility of regenerated aerosol particles.

	GTP (mm)				
Case name/solubility	F1	F05	F01	F001	FC
			Wet clean		
C_RH95_CTRL	163	166	172	189	168
C_RH95_SMD	96	107	144	185	95
C_RH95_BMD1	99	108	144	185	95
*	—	—	—	—	117
C_RH95_BMD2	108	112	144	185	95
			Dry clean		
C_RH85_CTRL	46	47	44	42	47
C_RH85_SMD	15	15	20	36	14
C_RH85_BMD1	15	15	20	37	14
*	—	—	—	—	18
C_RH85_BMD2	18	17	20	37	14
			Wet polluted		
P_RH95_CTRL	53	66	102	162	51
P_RH95_SMD	20	20	75	160	11
P_RH95_BMD1	30	21	75	160	11
*	—	—	—	—	14
P_RH95_BMD2	60	42	81	160	11
			Dry polluted		
P_RH85_CTRL	2.5	2.8	4.5	15	2.3
P_RH85_SMD	2.5	2.7	4.0	12	2.2
P_RH85_BMD1	2.5	2.7	4.0	12	2.2
*	—	—	—	—	2.4
P_RH85_BMD2	4.0	2.9	4.0	12	2.2

fewer regenerated aerosol particles than others, causing the lowest drop concentration in the second cloud. The very similar and low aerosol concentrations of different regenerated aerosol size distributions in F001 make the condensation process very active, which dominates the precipitation rates.

The investigation of effects of regenerated aerosol size distributions on the second cloud and precipitation reveals the following points: 1) When the aerosol solubility is high (50%–100%), the precipitation increases as a result of the increasing GCCN concentration associated with bimodal size distributions (see Table 4). This effect is more prominent for polluted clouds than for clean clouds. 2) When the aerosol solubility is very low (1%), the precipitation is insensitive to regenerated aerosol size distributions because of the similar and low CCN concentrations of these distributions. 3) When the aerosol solubility follows the function of FC, the precipitation is insensitive to regenerated aerosol size distributions because of the missing of GCCN and similar CCN concentrations of these distributions.

In addition to the effects of aerosol regeneration on clouds and precipitation, how clouds and precipitation redistribute aerosol particles in space through aerosol regeneration has also been investigated in this study. In these simulations, the dynamics is not a strong factor to redistribute the aerosol vertically. The cloud processing is then the critical element in controlling the aerosol redistribution. As shown in Figs. 9b and 10b, the regeneration increases the domain total drop number compared to the CTRL cases. Figure 11 illustrates how the horizontally integrated total number of aerosol particles greater than 0.1 μm is redistributed in vertical direction up to cloud top at 4 km as a function of time for the three representative solubilities discussed above. Most aerosols smaller than 0.1 μm stay as interstitial aerosol particles that do not affect clouds at all.

Both clean and polluted clouds with regeneration replenish background aerosol particles mostly above 800 m after 2 h. The smallest replenish rates of F001 reflect the lowest amount of activated aerosol particles in this case. The highest replenish rates of all cases around 4–7 h indicate that the evaporation of clouds over both hills reaches the maximum. The decreasing replenish rates after that period imply that the evaporation of the second cloud affected by regenerated aerosol particles becomes weaker than before, which is caused by the lower drop number in the cloud when regenerated aerosol particles reach it. Figure 11 shows that stronger evaporation occurs in higher altitudes in clean clouds than in polluted clouds and in the wet condition than in the dry condition (see the tight value contours in Fig. 11). This is the result of cloud tops that are associated with different thermodynamic conditions (see Fig. 5). In general, the regeneration of aerosol particles replenishes $^1/_3$–$^2/_3$ of the missing aerosol particles domainwise when regeneration is not considered. As a result, a more uniform aerosol background is achieved.

The effects of the modified solubility of regenerated aerosol particles by cloud processing on the second cloud and precipitation in the wet condition are illustrated in Fig. 12. The time series of total water mass, drop number, and precipitation rates of clean clouds are plotted for the modified solubility case, which is indicated by FC_F01, the FC and F01 cases. For polluted clouds, the modified solubility case (FC_F05), the FC and F05 cases are plotted. According to the experimental design of these modified solubility cases (see section 3b), the cloud features before regenerated aerosols reaching the second cloud should be exactly the same as FC cases, which has been verified by these figures (curves A and B overlap before 5 h).

Figure 12 shows that modifications of solubility of aerosol particles greater than 0.05 μm change little of the total water mass but reduce a significant amount of the total number of drops. The modified total number of drops is slightly higher than the F01 case for clean clouds and the F05 case for polluted clouds after 5 h because the number of regenerated aerosol particles of the FC_F01 and FC_F05 cases are greater than those of the F01

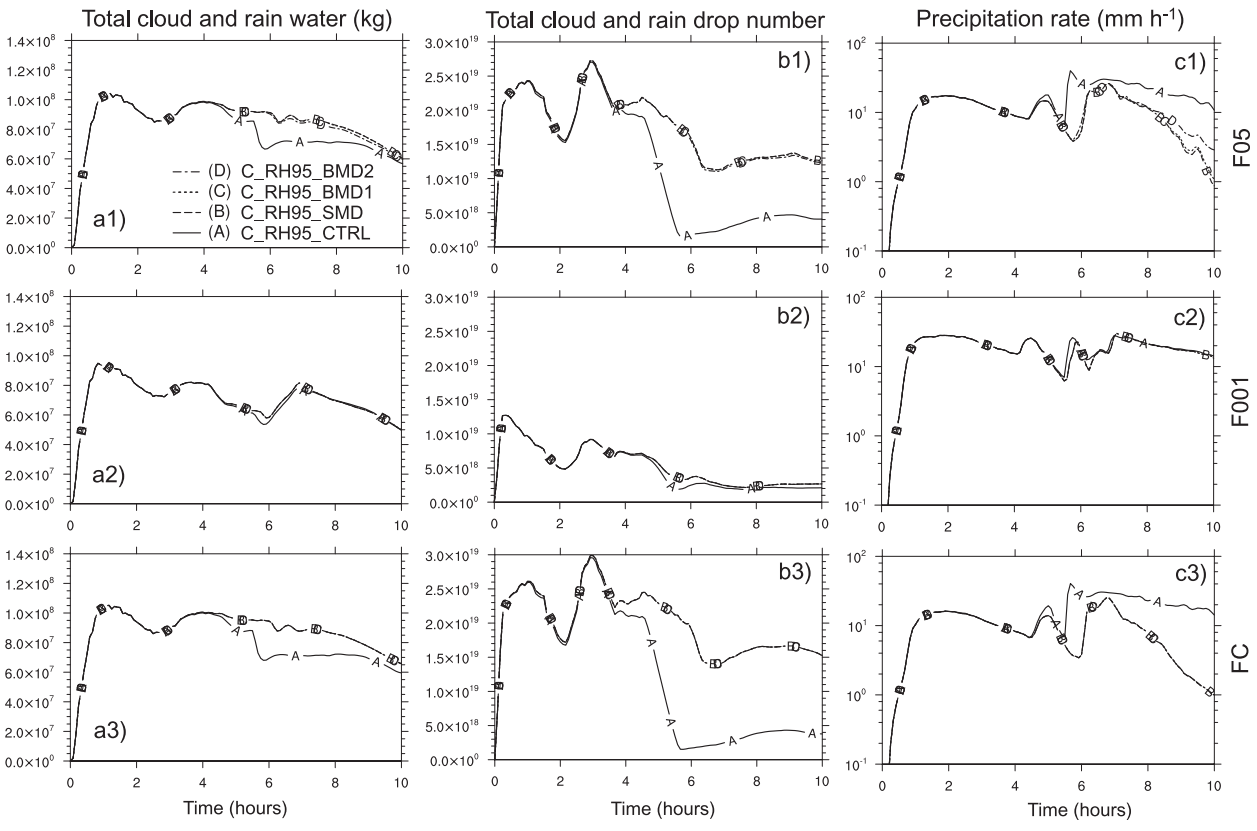

FIG. 9. As in Fig. 6, but for F05, F001, and FC cases of clean clouds in the wet condition.

(clean clouds) and F05 cases (polluted clouds) from the first clouds, which means more CCN are available in the second clouds for the FC_F01 and FC_F05 cases. As a result, the precipitation rate of the modified solubility case increases to a level close to the F01 case for clean clouds and close to the F05 case for polluted clouds. The modified solubility effect on the second cloud is similar in the dry condition. Therefore, the GTP of the second cloud with modified solubility of regenerated aerosol particles is between FC and F01 for clean clouds and between FC and F05 for polluted clouds (see Table 4).

Two more experiments have been carried out to test how the cutoff size of modification of solubility affects the result. In one experiment, the solubility of regenerated aerosol particles with radii greater than 1 μm is set to 0.1. In the other experiment, the solubility of regenerated aerosol particles with radii greater than 0.4 μm is set to 0.5. Both cases showed negligible effect on clouds and precipitation over the second hill for both clean and polluted cases. This result indicates that the solubility modification of regenerated aerosol particles with radii less than 0.4 μm is crucial to the second clouds.

It should be mentioned that the modified solubility effect of regenerated aerosol particles on the second clouds documented in this article is based on an aerosol solubility distribution described by Eq. (2) and Fig. 4. If the aerosol solubility distribution is very different from what we applied here, the effect might vary significantly or even reverse.

5. Summary and conclusions

The effects of aerosol solubility and regeneration on clouds and precipitation have been evaluated by simulating 2D idealized warm-phase cloud formation over two bell-shaped mountains using a detailed bin microphysical scheme embedded in WRF. A new drop activation submodule and an aerosol regeneration submodule have been implemented. Through changing water drop size distribution and adjusting subsequent microphysical processes, aerosol solubility and regeneration affect clouds and precipitation greatly.

The main results and conclusions of this aerosol–cloud–precipitation interactions study are summarized as follows:

1) The total number of cloud drops decreases as the aerosol solubility decreases. The impacts of aerosol solubility on cloud drops and precipitation are more significant in polluted clouds than in clean clouds.

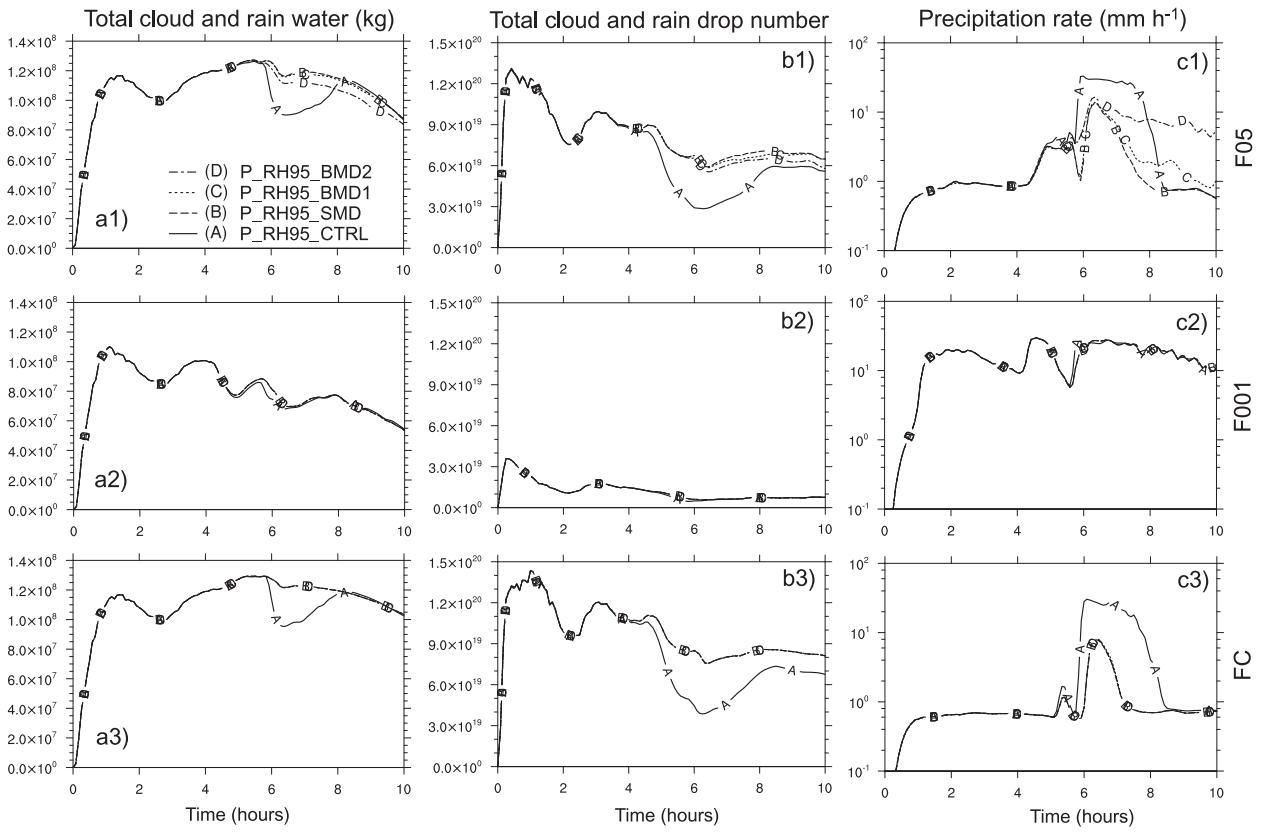

FIG. 10. As in Fig. 9, but for polluted clouds.

Aerosol solubility decides the CCN and GCCN concentrations given the same background concentration. High solubility leads to high CCN and high GCCN concentrations. When the moisture is plentiful, the strong activation by GCCN can initiate an efficient C–C process, resulting in abundant precipitation. But in the dry condition, high solubility results in less precipitation than low solubility cases. Very low solubility produces very few CCN, which leads to high supersaturation and thus strong condensation. The strong condensation generating plenty of large drops leads to an efficient C–C process and a great amount of precipitation. If the small aerosol particles have high solubility and large particles have low solubility, the CCN concentration is high and the GCCN concentration is low. As a result, very little precipitation is produced by the cloud. The sensitivities of clouds to aerosol solubility in this study agree qualitatively well with those simulated by cloud parcel model (Reutter et al. 2009). Our results also imply that to better quantify the aerosol solubility effect, the entire cloud system needs to be simulated by models with complete dynamics and microphysics. Figure 13 is a schematic that summarizes the effects of aerosol solubility on warm-phase orographic precipitation.

2) Aerosol regeneration increases cloud drops and reduces the precipitation by 2%–80% in clouds over the second mountain. Regenerated aerosol particles replenish $\frac{1}{3}$–$\frac{2}{3}$ of the missing particles when regeneration is not considered.

It is physically reasonable to represent aerosol regeneration in numerical models. Otherwise, much cleaner clouds, too much precipitation, and much less background aerosol particles will be simulated. Consideration of aerosol regeneration increases the sensitivities of cloud number concentration and precipitation to the aerosol solubility.

3) Different size distributions of regenerated aerosol particles have a negligible effect on clouds and precipitation except for polluted clouds with high aerosol solubility.

Similar to the effect of solubility on clouds and precipitation, the regenerated aerosol size distributions affect clouds by defining the CCN and GCCN concentrations. However, this effect is inferior to that of aerosol solubility because of the following two

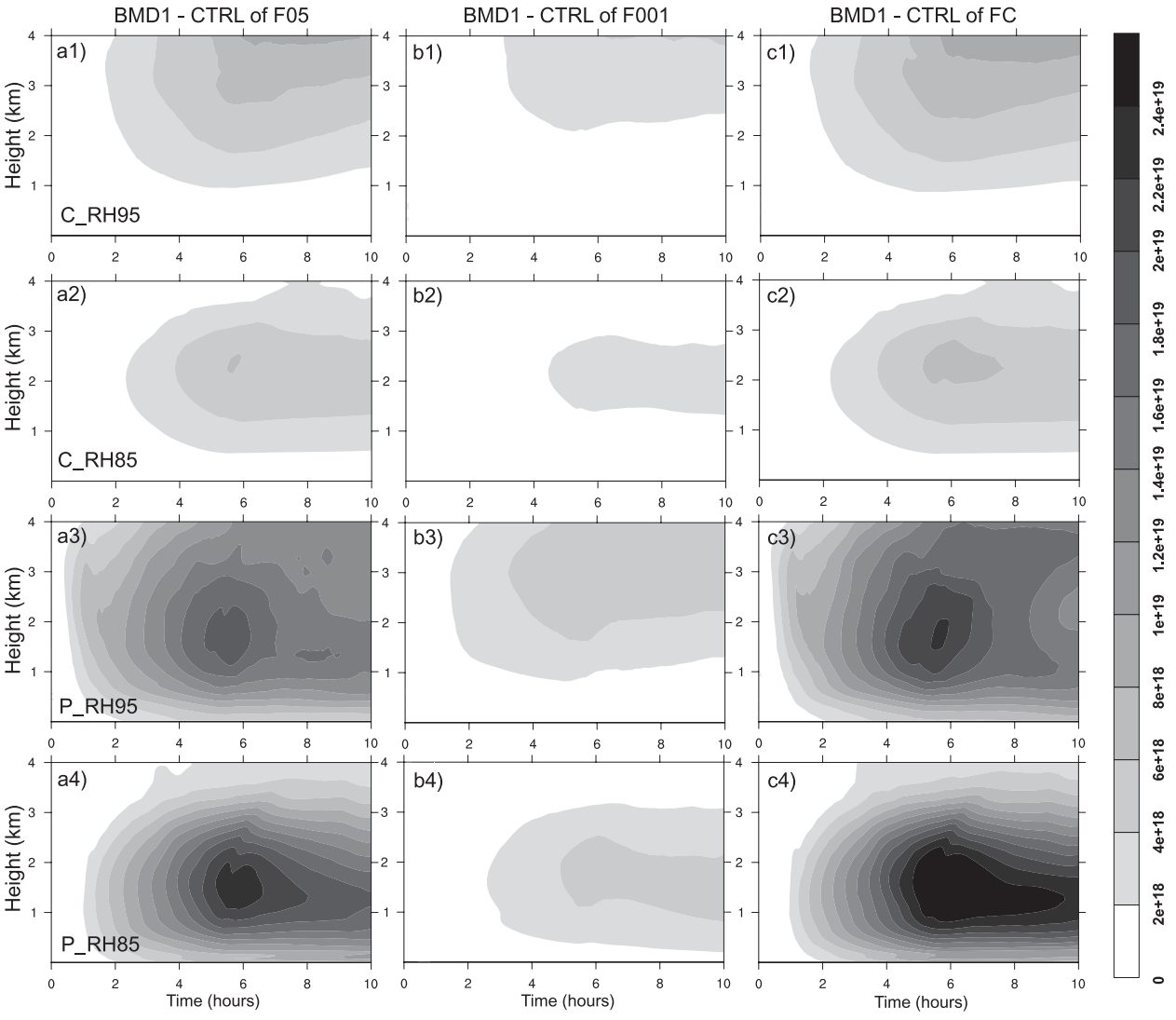

FIG. 11. Time–height contours of the differences of aerosol particles >0.1 μm between BMD1 and CTRL for the (a) F05, (b) F001, and (c) FC cases.

reasons: 1) the requirement of mass conservation of regenerated aerosol particles decides that the proportion of GCCN in the regenerated aerosol population is small, and 2) the fact that the amount of regenerated aerosol particles is less than the initial background value makes the second cloud cleaner, under which condition the GCCN effect is less prominent (e.g., Yin et al. 2000; Teller and Levin 2006). Only wet polluted clouds have a noticeable size distribution effect (GTP in BMD2 is about 2 times of that in SMD) when the solubility is high (100% and 50%).

4) In this study, when the solubility of the initial aerosol decreases with an increasing size of aerosol particles, the modified solubility of regenerated aerosol particles as a result of cloud processing increases precipitation over the second mountain.

The collision–coalescence process mixes the soluble and insoluble parts of aerosol particles inside each colliding drop into the coagulated drop. When the drop evaporates, the soluble materials will stick the other insoluble materials together as a single particle. This process increases the size and the solubility of the regenerated aerosol. When the solubility follows FC, the modified solubility of particles greater than 0.4 μm does not affect the cloud and precipitation.

A schematic of aerosol–cloud–precipitation interactions summarized from this study is illustrated in Fig. 14.

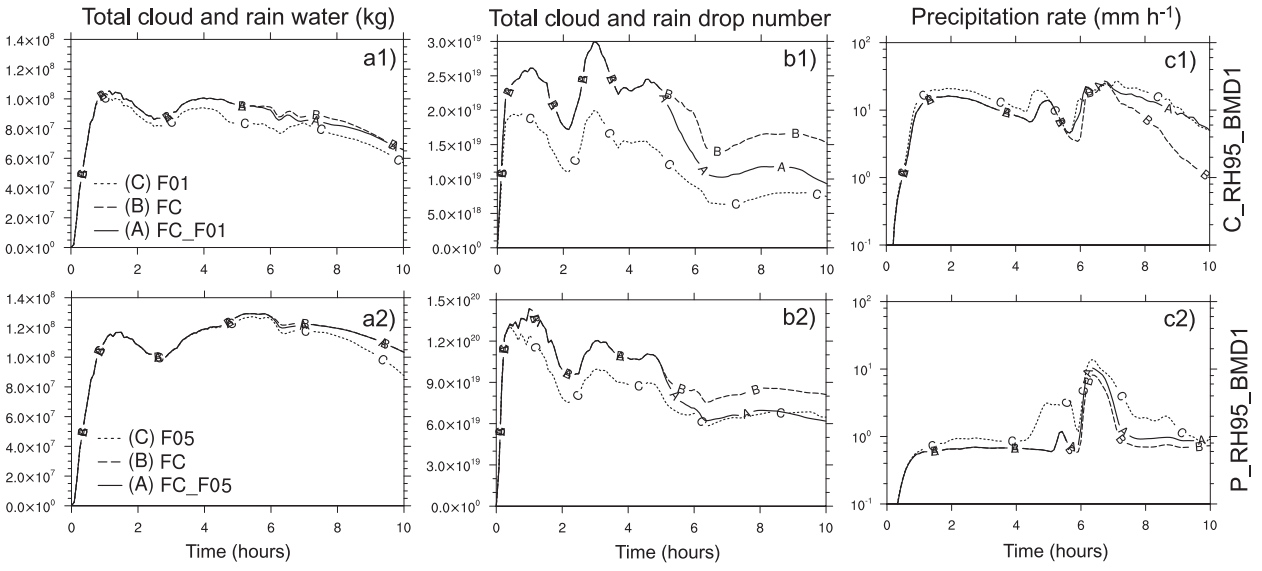

FIG. 12. As in Fig. 6, but for modified solubility of regenerated aerosol cases. Lines A–C represent the FC_F01, FC, and F01 cases for clean clouds and FC_F05, FC, and F05 cases for polluted clouds, respectively.

The initial aerosol population with different solubilities activates a cloud when conditions are favorable. Processed by the cloud, regenerated aerosol particles are released at the edge of the cloud by complete evaporation of cloud drops. The amount of these regenerated aerosol particles is less than that of the initial background value because some of the initial aerosol particles have been scavenged by the cloud and precipitation. These regenerated aerosol particles with modified solubility can activate new clouds and precipitation. Thus, a loop is

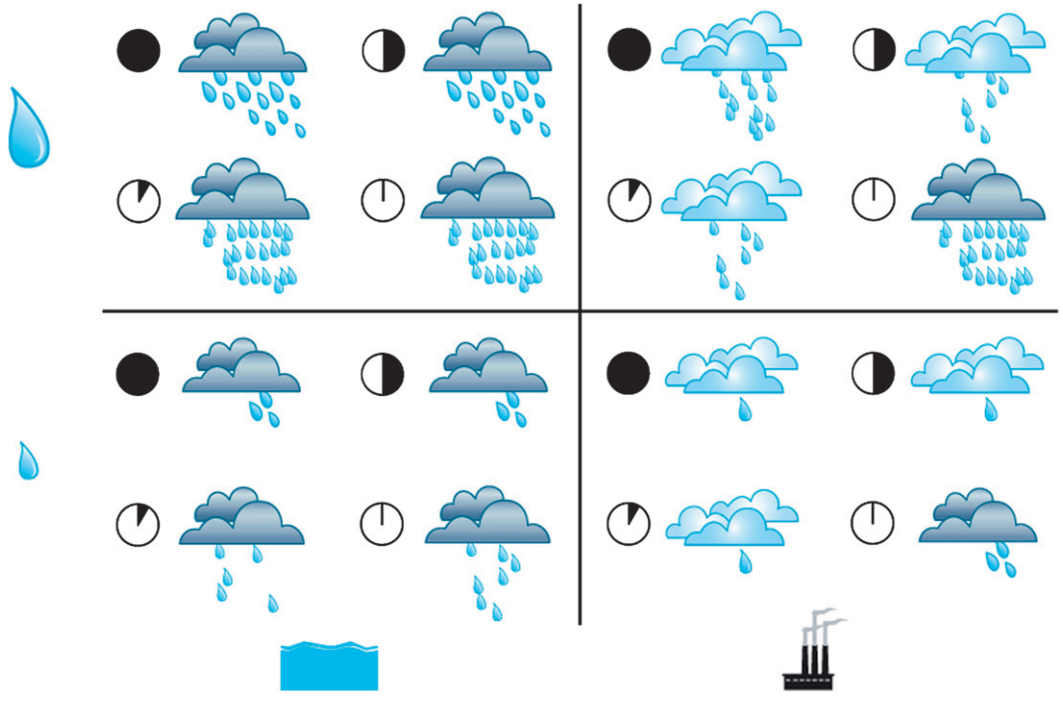

FIG. 13. Schematics of aerosol solubility effects on clouds and precipitation. Top and bottom quadrants indicate wet and dry conditions, respectively; left and right quadrants respectively indicate the clean and polluted backgrounds. Circles represent aerosol solubility of 100%, 50%, 10%, and 1%, with the black area indicating the soluble portion of the aerosol. Clean clouds are indicated by dark clouds and polluted clouds by the light ones.

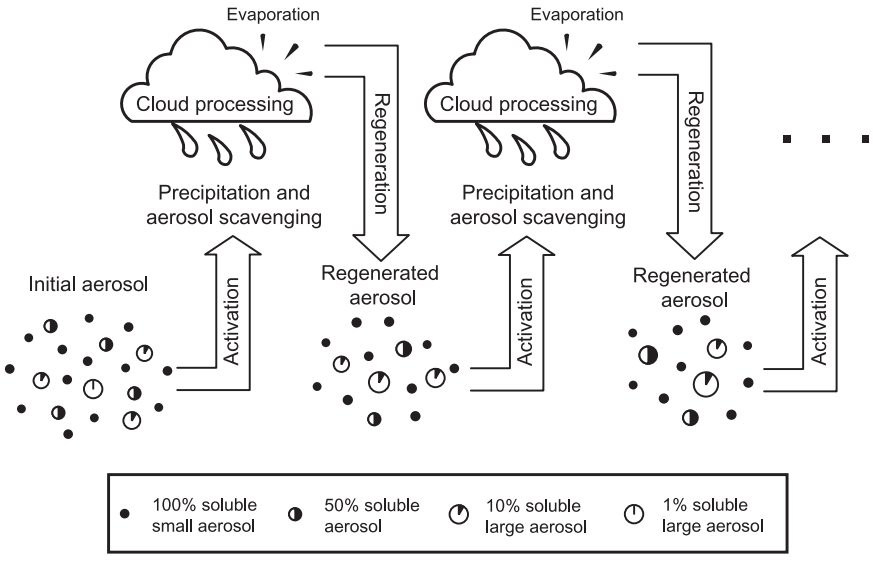

FIG. 14. Schematics of aerosol–cloud–precipitation interactions.

formed. The question of whether an equilibrium state of background aerosol exists or not will be explored in a future paper. The aerosol solubility and regeneration effects on mixed-phase orographic clouds are to be examined in the near future as well.

Acknowledgments. This study was partly supported by the National Institute for Climate Change Research (NICCR), Iowa Soybean Association, NCAR Advanced Study Program (ASP), and the Presidency of Meteorology and Environment (PME) in Saudi Arabia through a contract with Weather Modification Incorporated (WMI) of Fargo, North Dakota. The insightful comments from three anonymous reviewers are greatly appreciated by the authors. The authors would also like to thank Nichole McKinney for her technical editing of the manuscript in various versions.

REFERENCES

Ayers, G. P., 2005: Air pollution and climate change: Has air pollution suppressed rainfall over Australia? *Clean Air Environ. Quality,* **39,** 51–57.

Berg, L. K., and Coauthors, 2009: Overview of the cumulus humilis aerosol processing study. *Bull. Amer. Meteor. Soc.,* **90,** 1653–1667.

Engström, A., A. M. L. Ekman, R. Kerjci, J. Ström, M. de Reus, and C. Wang, 2008: Observational and modelling evidence of tropical deep convective clouds as a source of mid-tropospheric accumulation mode aerosols. *Proc. 15th Int. Conf. on Clouds and Precipitation,* Cancun, Mexico, ICCP, 3.6.

Feingold, G., 2003: Modeling of the first indirect effect: Analysis of measurement requirements. *Geophys. Res. Lett.,* **30,** 1997, doi:10.1029/2003GL017967.

——, and S. M. Kreidenweis, 2002: Cloud processing of aerosol as modeled by a large eddy simulation with coupled microphysics and aqueous chemistry. *J. Geophys. Res.,* **107,** 4687, doi:10.1029/2002JD002054.

——, S. Tzivion, and Z. Levin, 1988: Evolution of raindrop spectra. Part I: Solution to the stochastic collection/breakup equation using the method of moments. *J. Atmos. Sci.,* **45,** 3387–3399.

Flossmann, A. I., 1997: Interaction of aerosol particles and clouds. *J. Atmos. Sci.,* **55,** 879–887.

——, W. D. Hall, and H. R. Pruppacher, 1985: A theoretical study of the wet removal of atmospheric pollutants. Part I: The redistribution of aerosol particles captured through nucleation and impaction scavenging by growing cloud drops. *J. Atmos. Sci.,* **42,** 583–606.

Geresdi, I., 1998: Idealized simulation of the Colorado hailstorm case: Comparison of bulk and detailed microphysics. *Atmos. Res.,* **45,** 237–252.

——, and R. M. Rasmussen, 2005: Freezing drizzle formation in stably stratified layer clouds. Part II: The role of giant nuclei and aerosol particle size distribution and solubility. *J. Atmos. Sci.,* **62,** 2037–2057.

Hall, W. D., 1980: A detailed microphysical model within a two-dimensional framework: Model description and preliminary results. *J. Atmos. Sci.,* **37,** 2486–2507.

Hobbs, P. V., 1993: *Aerosol–Cloud–Climate Interactions*. Academic Press, 233 pp.

Jaenicke, R., 1988: Aerosol physics and chemistry. *Physical and Chemical Properties of the Air,* G. Fischer, Ed., Landolt-Bömstein New Series, Vol. 4b, Springer, 391–457.

Khain, A. P., N. BenMoshe, and A. Pokrovsky, 2008: Factors determining the impact of aerosols on surface precipitation from cloud: An attempt at classification. *J. Atmos. Sci.,* **65,** 1721–1748.

Kogan, Y. L., 1991: The simulation of a convective cloud in a 3D model with explicit microphysics. Part I: Model description and sensitivity experiments. *J. Atmos. Sci.,* **48,** 1160–1189.

Laj, P., and Coauthors, 1997: Experimental evidence for in-cloud production of aerosol sulphate. *Atmos. Environ.,* **31,** 2503–2514.

Lance, S., A. Nenes, and T. A. Rissman, 2004: Chemical and dynamical effects on cloud droplet number: Implications for estimates of the aerosol indirect effect. *J. Geophys. Res.,* **109,** D22208, doi:10.1029/2004JD004596.

Lynn, B., A. Khain, D. Rosenfeld, and W. L. Woodley, 2008: Effects of aerosols on precipitation from orographic clouds. *J. Geophys. Res.,* **112,** D10225, doi:10.1029/2006JD007537.

McFiggans, G., and Coauthors, 2006: The effect of physical and chemical aerosol properties on warm cloud droplet activation. *Atmos. Chem. Phys.,* **6,** 2593–2649.

Mitra, S. K., J. Brinkmann, and H. T. Pruppacher, 1992: A wind tunnel study on the drop-to-particle conversion. *J. Aerosol Sci.,* **23,** 245–256.

Morrison, H., G. Thompson, M. Gilmore, W. Gong, R. Leaitch, and A. Muhlbauer, 2009: WMO International Cloud Modeling Workshop. *Bull. Amer. Meteor. Soc.,* **90,** 1683–1686.

Muhlbauer, A., and U. Lohmann, 2008: Sensitivity studies of the role of aerosol in warm-phase orographic precipitation in different dynamical flow regimes. *J. Atmos. Sci.,* **65,** 2522–2542.

——, T. Hashino, L. Xue, A. Teller, U. Lohmann, R. M. Rasmussen, I. Geresdi, and Z. Pan, 2010: Intercomparison of aerosol–cloud–precipitation interactions in stratiform orographic mixed-phase clouds. *Atmos. Chem. Phys. Discuss.,* **10,** 10 487–10 550.

Petters, M. D., and S. M. Kreidenweis, 2007: A single parameter representation of hygroscopic growth and cloud condensation nucleus activity. *Atmos. Chem. Phys.,* **7,** 1961–1971.

Pruppacher, H. R., and R. Jaenicke, 1995: The processing of water vapor and aerosols by atmospheric clouds, a global estimate. *Tellus,* **38,** 283–295.

——, and J. D. Klett, 1997: *Microphysics of Clouds and Precipitation*. Kluwer Academic, 954 pp.

Rasmussen, R. M., I. Geresdi, G. Thompson, K. Manning, and E. Karplus, 2002: Freezing drizzle formation in stably stratified layer clouds: The role of radiative cooling of cloud droplets, cloud condensation nuclei, and ice initiation. *J. Atmos. Sci.,* **59,** 837–860.

Reisin, T., Z. Levin, and S. Tzivion, 1996: Rain production in convective clouds as simulated in an axisymmetric model with detailed microphysics: Part I. Description of the model. *J. Atmos. Sci.,* **53,** 497–519.

Reutter, P., and Coauthors, 2009: Aerosol- and updraft-limited regimes of cloud droplet formation: Influence of particle number, size and hygroscopicity on the activation of cloud condensation nuclei (CCN). *Atmos. Chem. Phys.,* **9,** 7067–7080.

Roe, G. H., 2005: Orographic precipitation. *Annu. Rev. Earth Planet. Sci.,* **33,** 645–671.

Rosenfeld, D., 2000: Suppression of rain and snow by urban and industrial air pollution. *Science,* **287,** 1793–1796.

Skamarock, W. C., and Coauthors, 2008: A description of the Advanced Research WRF version 3. NCAR Tech. Rep. NCAR/TNC-475+STR, 113 pp.

Solomon, S., D. Qin, M. Manning, M. Marquis, K. Averyt, M. M. B. Tignor, H. L. Miller Jr., and Z. Chen, Eds., 2007: *Climate Change 2007: The Physical Science Basis*. Cambridge University Press, 996 pp.

Teller, A., and Z. Levin, 2006: The effects of aerosols on precipitation and dimensions of subtropical clouds: A sensitivity study using a numerical cloud model. *Atmos. Chem. Phys.,* **6,** 67–80.

Thompson, G., R. Rasmussen, and K. Manning, 2004: Explicit forecasts of winter precipitation using an improved bulk microphysics scheme. Part I: Description and sensitivity analysis. *Mon. Wea. Rev.,* **132,** 519–542.

Tzivion, S., G. Feingold, and Z. Levin, 1987: An efficient numerical solution to the stochastic collection equation. *J. Atmos. Sci.,* **44,** 3139–3149.

——, T. Reisin, and Z. Levin, 1999: A numerical solution of the kinetic collection equation using high spectral grid resolution: A proposed reference. *J. Comput. Phys.,* **148,** 527–544.

van den Heever, S. C., G. Carrio, W. R. Cotton, P. J. DeMott, and A. J. Prenni, 2006: Impacts of nucleating aerosol on Florida convection. Part I: Mesoscale simulations. *J. Atmos. Sci.,* **63,** 1752–1775.

Wang, H., W. C. Skamarock, and G. Feingold, 2009: Evaluation of scalar advection schemes in the Advanced Research WRF model using large-eddy simulations of aerosol–cloud interactions. *Mon. Wea. Rev.,* **137,** 2547–2558.

Wurzler, S., T. G. Reisin, and Z. Levin, 2000: Modification of mineral dust particles by cloud processing and subsequent effect on drop size distributions. *J. Geophys. Res.,* **105,** 4501–4512.

Yin, Y., Z. Levin, T. G. Reisin, and S. Tzivion, 2000: The effects of giant cloud condensation nuclei on the development of precipitation in convective clouds—A numerical study. *Atmos. Res.,* **53,** 93–116.

——, K. S. Carslaw, and G. Feingold, 2005: Vertical transport and processing of aerosols in a mixed-phase convective cloud and the feedback on cloud development. *Quart. J. Roy. Meteor. Soc.,* **131,** 221–245.